



Compounding sub-seasonal variations in Greenland outlet glacier dynamics revealed by high-resolution observations

Enze Zhang^{1,3}, Ginny Catania^{1,2}, Ben Smith⁴, Denis Felikson⁵, Beata Csatho⁶, and Daniel T. Trugman⁷

Correspondence: Ginny Catania (gcatania@jsg.utexas.edu)

Abstract. Understanding the controls on seasonal velocity change for tidewater glaciers may provide insight into long-term retreat and acceleration. Leveraging recent high-resolution satellite data, we examine changes in surface elevation, velocity, and terminus position for four glaciers in Central Western Greenland over 2015-2021. Our approach uses a simplified force balance focused at the terminus and to model the expected response in upstream velocity caused by the observed terminus changes. We find that seasonal velocities are strongly controlled by terminus advance/retreat for two glaciers. Residuals between modeled and observed velocities reveal other velocity signals including summertime pulses that are coincident with periods of high runoff and wintertime speedup that extends several kilometers inland of the terminus. We test the sensitivity of our results by including observed seasonally varying surface topography and making artificial modifications, such as shifting the entire profile and altering surface slope. We find surface slope changes impact velocity response to terminus changes more than spatially uniform changes in elevation. Increased surface slope amplifies velocity response to terminus changes. While simplified, our model could be applied to other glaciers to assess the importance of terminus position change as a driver of seasonal velocity.

1 Introduction

The Greenland Ice Sheet (GrIS) is currently the largest land ice contributor to present-day rising sea level (IPCC, 2022) with an acceleration in mass loss over the past few decades largely attributed to ice discharge through outlet glaciers (Shepherd et al., 2012; Enderlin et al., 2014; van den Broeke et al., 2016). This acceleration underscores the importance of comprehending the intricate mechanisms that govern glacier dynamics. Despite the prevalence of glacier acceleration in Greenland, there exists notable spatio-temporal variability in glacier velocity change at a range of time scales (Moon et al., 2012, 2020; Black and Joughin, 2023). This is likely because glacier velocity is influenced by local conditions, like topography, and regionally by environmental factors. For example, runoff and ocean thermal forcing can influence velocity by changing basal friction (Ultee

¹The University of Texas at Austin, Institute of Geophysics, TX, USA

²The University of Texas at Austin, Department of Geological Sciences, TX, USA

³The Hong Kong University of Science and Technology, Department of Civil and Environmental Engineering, Hong Kong, China

⁴Polar Science Center, Applied Physics Laboratory, University of Washington, Seattle, WA, USA

⁵Cryospheric Sciences Laboratory, NASA Goddard Space Flight Center, Greenbelt, MD, USA

⁶Department of Geological Sciences, University at Buffalo, Buffalo, NY, USA

⁷Nevada Seismological Laboratory, Nevada Geosciences, University of Nevada, Reno, NV, USA





et al., 2022), subaqueous melt rates (Holland et al., 2008), and through terminus fluctuations (Howat et al., 2008; King et al., 2020; Wood et al., 2021).

Outlet glaciers in Greenland present seasonal velocity changes (Moon et al., 2015; Joughin et al., 2008; King et al., 2018), but it is not clear what exact process is involved. In part, this is because many of the processes that influence outlet glacier velocity are synchronized, making it difficult to disentangle cause and effect. Some studies have suggested increased air temperature leads to summertime melting and terminus retreat, which reduces ice contact with the bed and/or fjord walls and increases net force at the calving cliff, both driving glacier acceleration (Howat et al., 2005; Joughin et al., 2012). Numerical simulations also suggest a non-linear feedback between the rate of terminus change and ice discharge (Sergienko, 2022). Others have indicated that glacier acceleration is due to seasonal changes in basal lubrication related to changes in the subglacial hydrological system (Davison et al., 2020; Stevens et al., 2022; Werder et al., 2013; Andrews et al., 2014), which can cause complex responses in glacier velocities as subglacial conduits grow more efficient (Bartholomew et al., 2010; Andrews et al., 2014; Vijay et al., 2019).

Understanding seasonal drivers of glacier change may help researchers to understand longer term glacier changes. Moreover, numerical simulations suggest that seasonal changes can induce systematic bias in mass loss estimates at the multi-decadal time scale, compared to simulations that do not include seasonal forcing, because the magnitude of mass loss is higher during retreat than mass gain for an equal amount of advance (Felikson et al., 2022; Robel et al., 2018). Thus, investigating the patterns of glacier seasonality may be critical to unveiling the factors that control glacier dynamics into the future.

Previous efforts have classified glacier seasonal velocity variations into types based on the observed timing of velocity change and their correlation to runoff and terminus change (Moon et al., 2014; Vijay et al., 2019, 2021). This classification enhances our understanding of the factors that drive these seasonal variations. Three categories have been generally described in Moon et al. (2014): type-1 has positive correlation of glacier velocity to glacier terminus retreat; type-2 has positive correlation of glacier velocity to summer runoff, and; type-3 shows glacier velocity that slows in late summer and speeds up in winter. In a subsequent study, Vijay et al. (2019) employed high temporal resolution velocity data, terminus changes, and radar-backscatter intensity values to classify 45 glaciers into the same three types. Vijay et al. (2021) extended their previous analysis to encompass 221 glaciers across the entirety of Greenland but their classification of these glaciers still resulted in two distinct types. Solgaard et al. (2022) combined both velocity and runoff data, and employed a machine-learning approach to classify glaciers throughout Greenland. Their findings revealed similar seasonal patterns as those initially identified by Moon et al. (2014). Finally, Poinar (2023) applied principal component analysis to decompose the seasonality of glaciers in Sermilik Fjord from a statistical perspective. They classified four glaciers in Sermilik Fjord by quantifying the prevalence of multiple seasonality types at a single glacier. Furthermore, they emphasized the importance of extracting velocity patterns across the entire glacier, not just a single point. While these studies have made significant contributions to glacier classification and understanding seasonal behavior, the majority of them do not examine how the compounding effects of various processes influence seasonal glacier velocity. Moreover, none have incorporated a physics-based model in their analysis. Due to limitations in temporal resolution, these studies classified glacier behavior within a year as a single category. However, glaciers can experience multiple influences simultaneously or sequentially within a season, leading to compounding dynamic behaviors.





Here, we re-examine glacier seasonality using high-frequency terminus (Zhang et al., 2023), velocity (Gardner et al., 2023), and surface elevation change observations for four glaciers in Greenland. We interpret these observations with an analytical model of velocity response to terminus position change (Joughin et al., 2012). While simple, this model provides a physics-based method to decouple the myriad processes that influence ice velocity by removing one potential driver - terminus change. By isolating the velocity component that is driven by terminus changes, we find that glaciers are more typically influenced by an interplay of multiple processes simultaneously or sequentially rather than a single process during a single season. By utilizing high temporal resolution data in this study, we can more accurately decompose how different processes affect glacier velocity throughout a season, identifying the sub-seasonal characterization of velocity, which may be more appropriate for the classification of glacier velocity.

2 Study region

We investigate four glaciers in central-west Greenland (Figure 1): Sermeq Avannarleq (AVA), Sermeq Kujalleq (KUJ), Kangilernata Sermia (KAN), and Eqip Sermia (EQP) over the time period 2015-2021. This time span is specifically chosen to take advantage of the increased sample frequency available in both velocity and terminus position data due to the launch of Sentinel-1/2 in April 2014, which offers full year coverage of velocity data. We choose these 4 glaciers because we want to understand how our simple model might aid interpretation of seasonal velocity change for glaciers that have been extensively studied in the past. These glaciers are selected because they 1) are well-grounded; 2) exhibit regular seasonal changes in both terminus position and velocity with minimal long-term variations over our study period (Catania et al., 2018; Fried et al., 2018) and; 3) exhibit a range of sub-seasonal behavior in both the terminus and velocity variability. As a result, these four glaciers likely represent the majority of other well-grounded outlet glaciers in Greenland experiencing seasonal change. For example, all glaciers advance in winter and retreat in summer and yet their seasonal velocity behavior differs over time and space. EQP and KUJ speed up during summertime terminus retreat while AVA and KAN slow down during summertime terminus retreat (Fried et al., 2018). In addition, AVA, KUJ, KAN, and EQP are located close to one another, suggesting that they likely experience the same regional climate forcing, they also exhibit distinct local effects, such as geometry that impact their dynamic behaviors. For instance, EQP's steep slope results in higher glacier velocities and more frequent calving events (LÜTHI et al., 2016; Kneib-Walter et al., 2023), whereas the shallow sills of AVA and KUJ contribute to their remarkable stability over the past century (An et al., 2018).

These glaciers have been studied extensively by previous authors. All glaciers have been relatively stable (they have not retreated more than the amplitude of seasonal fluctuations) since 2015 (Table 1). All four glaciers have experienced terminus retreat over the more extensive satellite era; AVA 0.64 km, KUJ 1.80 km, KAN 2.65 km, and EQP 2.54 km from 1999 to 2016(Catania et al., 2018). Studies of calving style for these glaciers indicate that they all primarily calve via serac failure due to undercutting related to terminus melt (Kneib-Walter et al., 2021; Bézu and Bartholomaus, 2024; Goliber and Catania, 2024), although KUJ has been reported to have a mix of serac failure and buoyant flexure calving styles (Bézu and Bartholomaus, 2024). This suggests that AVA, KAN, and EQP are well-grounded and that KUJ may approach floatation at times or in smaller





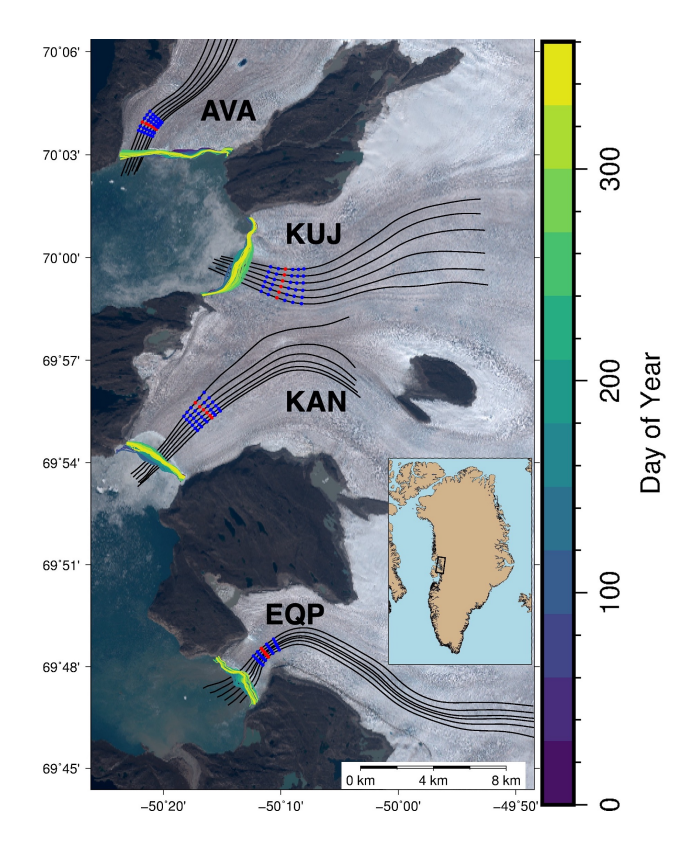


Figure 1. Glacier and data locations. Glaciers examined in this study include Sermeq Avannarleq (AVA), Sermeq Kujalleq (KUJ), Kangilernata Sermia (KAN), and Eqip Sermia (EQP). The terminus traces in 2018 from AutoTerm are colored by date. The red points show the locations where ITS_LIVE velocities were extracted for the model comparison in the results section. Blue points are the locations where we tested the sensitivity of the location of the velocity observation to the results. Blue and red points mark the locations for velocities shown in Supplemental Figures S2-S7.

regions of the terminus. This is consistent with an earlier study finding that these four glaciers experience terminus change that is predominantly driven by changes in subglacial runoff (Fried et al., 2018). Additional details on each glacier can be found in Table 1.

3 Data

90

We use velocity time series data generated using auto-RIFT (Gardner et al., 2018) and provided by the NASA MEaSURES ITS_LIVE project (Gardner et al., 2023). ITS_LIVE combines velocity products derived from Landsat-8, Sentinel-1, and Sentinel-2 and produces velocity data with a spatial resolution of 240 m. The number of velocity observations per month ranges from 18 to 19 for the four glaciers (Table 1). For each glacier, we use six flowlines across the glacier from Felikson et al. (2021) to extract velocities at six points along each flowline (red and blue points in Figure 1). We then average these velocities



105

110



Table 1. Summary of statistics for observations used, glacier geometry, and simulation results.

Glacier Name		KUJ	EQP	KAN	AVA
Glacier Width	(km)	5	3	4	6
Glacier Frontal Depth	(m)	421	134	403	399
Average velocity	(m/yr)	3699	1558	1178	1905
Terminus observations per month		14	11	13	14
Velocity observations per month		18	19	19	19
Velocity Uncertainty	(m/yr)	124	109	108	99
Terminus Uncertainty	(m/yr)	23	16	13	17
Model Velocity Uncertainty	(m/yr)	62	50	45	9
Distance of the Glacier Terminus to the Sampling Location	(km)	1.5	2	3.4	1.7
Glacier retreat rate	(m/yr)	10	24	11	10
Seasonal Terminus Change	(meters)	400	217	370	138
Seasonal Velocity Change	(m/yr)	853	359	404	862
Seasonal Simulated Velocity Change	(m/yr)	809	331	260	65
Coupling Length	(km)	20	10	N/A	N/A
Average Misfit between Simulated and Observed Velocity		5.0%	6.20%	14.2%	63.1%

across all flowlines at each cross section to produce mean (across-flow) velocity time series from downstream to upstream for each glacier. The flowlines of AVA predominantly converge on the western side of the basin because AVA is formed by the confluence of two upstream tributaries, and we focus on the main tributaries with higher velocities on the western side. Blue points in Figure 1 are used to test the model sensitivity to distance from the terminus as described in the Supplementary Information. We applied a 40-day rolling average to improve the visualization of the time series, as the original data was noisy. To compensate for the phase shift introduced by the rolling average, we shifted the time series back by 20 days. The rolling average was used only for visualization; all statistical analyses, including correlations and residuals, were conducted without it. To ensure the quality of the ITS_LIVE velocity data, we filter out measurements with dt greater than 45 days, where dt represents the interval between two scenes used to obtain glacier velocities. In addition to ITS_LIVE velocity data, we also extract along-flow velocity profiles from monthly velocity mosaics provided by the Greenland Ice Sheet Mapping Project (GrIMP) (Joughin, 2023) with a spatial resolution of 30 m. These along-flow profiles are exclusively used to examine the spatial pattern of velocity changes over seasons (Figure 10), while all velocity time series observations are sourced from ITS_LIVE velocity data.

Terminus position data come from AutoTerm (Zhang et al., 2023), a machine learning pipeline that automatically produces terminus traces with an average sampling frequency of 10 per month since 2014. We derive a time series of terminus change by calculating the sequential area changes between termini, accumulating these over time, and then normalizing this by a static glacier width of 6 km for AVA, 5 km for KUJ, 4 km for KAN, and 3 km for EQP. We apply the same 40-day rolling average





to smooth terminus data as described above. The uncertainties for ITS_LIVE, AutoTerm data, and simulated velocity from the terminus-driven model are represented as shaded areas in our time series figures (Figures 2 to 5) and we present the average uncertainties in Table 1.

We generate surface elevation data through a novel fusion of ICESat-2 data with DigitalGlobe high-resolution digital elevation models (DEMs), termed "DG-IS2-DEM" producing four DEMs per year from Fall 2018. The algorithms that generate the DG-IS2-DEMs are described in the Supplementary Information. We also use ArcticDEM (Porter et al., 2022) as supplementary elevation data in locations where the DG-IS2-DEMs do not extend to the most advanced terminus position found in AutoTerm. To determine ice thickness, we subtract surface elevation data from bed elevation data from BedMachineV5 (Morlighem et al., 2022), which assimilates seafloor bathymetry and ice thickness data through a mass conservation approach (Morlighem et al., 2017). BedMachine is an estimate of the bed topography, not a measurement and carries a spatial resolution of 150 m and uncertainties of \sim 60 m for AVA, \sim 70 m for KUJ, \sim 20 m for KAN, and \sim 90 m for EQP. These low uncertainties result because each of these glaciers have radar-determined bed elevation data to within \sim 1 km of the current terminus position (Catania et al., 2018). For both of these data sets we extract the elevation profiles along each flowline individually.

We use GSFC-FDMv1.2.1 simulations of the surface mass balance (Medley et al., 2022) to produce a runoff time series with a five-day sampling frequency at points in Figure 1. We use the onset and cessation of runoff as a proxy for the timing of the melt season. We choose to represent values of runoff that are less than 2 m/yr as winter time and values of runoff greater than 2 m/yr as summer time (Figures 2-5).

4 Terminus-Driven model

130

135

145

Force balance methods can be used to understand the dynamic evolution of glaciers by examining the balance of stresses on them (van der Veen et al., 2011; Carnahan et al., 2022). However, the force balance method requires a second-order derivative of surface velocity data, which can result in large uncertainties when using satellite products. Therefore, we adopt a different approach that employs a modified force balance termed the "terminus-driven model" described by Joughin et al. (2012). This model explicitly considers the influence of dynamic changes at the glacier terminus on upstream velocity. By using the terminus-driven model and near daily velocity data, we are able to isolate the contribution of terminus variations to the observed variations in the velocity time series. The terminus-driven model is a 1-D model along the flow direction, assuming ice mélange-free conditions, a constant glacier geometry over time, and a grounded glacier. The terminus-driven model first quantify the driving stress (τ_d) at the points where we simulate velocity, expressed as

$$\tau_d = -\rho_i g H \frac{\partial h}{\partial x} \tag{1}$$

where ρ_i is the density of ice (910 kg/m³), g is the gravitational acceleration (9.81 m/s²), H is ice thickness, h is ice surface elevation, x is the distance along the flowline with the direction from downstream to upstream. The driving stress is only calculated at the points where we simulate velocity. Secondly, the terminus-driven model examines an additional force at the water-terminating calving face, determined by the height above the fjord surface at the calving front and the density of seawater.



160



The difference between these two forces at the terminus is expressed as

$$F = \frac{1}{2}\rho_i gH^2 - \frac{1}{2}\rho_w g(H - h)^2$$
 (2)

where ρ_w is the density of seawater (1028 kg/m³). Here, we call F the "frontal force" following the naming convention found in Joughin et al. (2012), although it has units of N/m. The force balance at the terminus requires the frontal force to be balanced upstream by the longitudinal stress, which redistributes much of the frontal force to the glacier upstream. We term the longitudinal stress in the upstream region that originates from the frontal force as $\tau_F(X)$, which pulls/opposes the glacier and enhances/reduces the original driving stress (e.g., $\tau_d + \tau_F(X)$). X is the distance between terminus and the point where we simulate velocity.

The integration of $\tau_F(X)$ along the flowline equals F and is assumed to linearly decrease upstream of the terminus to zero at the stress coupling length following Joughin et al. (2012):

$$\tau_F(X) = 2\frac{F}{\lambda} \left(1 - \frac{X}{\lambda} \right) \tag{3}$$

where λ is the stress coupling length. Terminus variations cause changes in the geometry at the free calving face, consequently influencing the frontal force (F). These changes in the frontal force, subsequently, lead to modifications in the enhanced driving stress $(\tau_d + \tau_F(X))$ in the upstream region. Thus, the calculation of F and $\tau_F(X)$ over time requires elevation data along the profile.

In the laminar flow model or the shallow ice approximation, when basal sliding is zero, the surface velocity has a linear relationship with the cube of driving stress (n = 3):

$$V = \frac{1}{2}AH\tau_d^3 \tag{4}$$

where A is a constant from Glen's flow law (van der Veen, 2013) and V is surface velocity. Such a linear relationship also applies when the driving stress is mainly balanced by lateral drag (van der Veen, 2013):

$$V = \frac{1}{2}A\left(\frac{\tau_d}{H}\right)^3 W^4 \tag{5}$$

where W is half of the glacier width. Based on the above two models and following the method designed by Joughin et al. (2012), we assume a linear relationship between velocity and the cube of the enhanced driving stress: $\tau_d + \tau_F(X)$. Finally, the predicted velocity from terminus changes is thus given by:

170
$$\frac{V(X,t)}{V_0} = \left(\frac{\tau_d + \tau_F(X)}{\tau_d + \tau_{F_0}}\right)^3$$
 (6)

where V_0 is a reference velocity at the same location as velocity observations and τ_{F_0} is the $\tau_F(X)$ corresponding to the reference velocity. Following Joughin et al. (2012), for each year, we use the minimum velocity observation as the reference velocity and calculate τ_{F_0} based on the terminus position nearest the date of the reference velocity. Using Eqn. 6, we simulate velocity observations at both the blue and red points in Figure 1 using corresponding geometry profiles along each flowline.





175 Then, we average the simulated velocity across all the flowlines at each cross-section to produce mean velocity time series in a manner consistent with the observed velocity.

We vary stress coupling lengths for each glacier and choose the one that produces the lowest mean difference between observations and simulated velocity (Table S1). The mean difference is determined by:

$$\left(\sum_{n}^{N}\sum_{m}^{6}\frac{abs(V_{m,n}^{model}-V_{m,n}^{obs})}{V_{m,n}^{obs}}\right) \div (N\times6)\times100\%$$
(7)

80 where 6 is the total number of velocity points on the same cross section and N is the total number of time steps in the entire time series. We use the red points in Figure 1 to find an optimal stress coupling length. The optimized stress coupling lengths are then used to simulate velocity time series at the blue points in Figure 1, which allow us to test the sensitivity of the velocity position to the results.

We also calculate the velocity residual by subtracting the simulated velocity with fixed geometry from the observed velocity.

The velocity residual refers to the portion of the velocity that is not associated to terminus changes but is affected by other factors, such as runoff. We then plot residuals overlapping with runoff for ease of comparison (Figures 2-5). We assign the uncertainty of the terminus change (Zhang et al., 2023) as the error of *X* in Eqn. 3, and propagate this error to obtain the uncertainty in the simulated velocity. This uncertainty may be underestimated because we only account for uncertainties from the terminus data and not from elevation data, which also contributes to the errors of simulated velocity.

Although the terminus-driven model was initially designed by Joughin et al. (2012) to assume invariant geometry in its operation, we analytically examine the impact of seasonal variations in surface elevation on velocity simulations. Specifically, we leverage the new time-varying DG-IS2-DEM and periodically update the elevation profiles each quarter from Fall 2018, maintaining profile fixed within each quarter. We produce a simulated velocity for all glaciers with and without time-varying surface elevation in order to evaluate the impact of seasonally-varying surface elevation change on velocity. For the fixed geometry simulations, we choose a time step from DG-IS2-DEM with an extent that aligns best with the position of the terminus when it is most advanced. This provides the most complete elevation profile across the terminus region. For EQP, KAN, and AVA we choose the October 2019 DG-IS2-DEM and for KUJ, we use the April 2019 DG-IS2-DEM time step. To further investigate the impact of changing elevation on the simulation results, we consider only KUJ as an example and conduct two experiments using artificially modified surface elevation; 1) we shift the entire elevation profile vertically by ± 10 -20 m and; 2) we alter the surface slope by $\pm 2\%$ within the 2 km-frontal region.

5 Results

190

195

200

205

Our comparative analysis of model outputs, runoff data, and velocity observations reveals that the seasonal velocity variations of all four glaciers are influenced by three distinct processes, which align with those identified by Moon et al. (2014). We find that each glacier is affected by two of these processes, influencing glacier velocity either alternately or simultaneously each year. Following the classification by Moon et al. (2014), we categorize each glacier as follows: EQP and KUJ are classified as type-1 plus type-2, whereas KAN and AVA are classified as type-2 plus type-3. This classification differs from Vijay et al. (2021),



210

235



which classified EQP and KAN as type-3, identified AVA as type-2 in 2018 and type-3 in 2017 and 2019, and did not classify KUJ. The integration of high temporal resolution observations with a simplified physical model facilitates a more precise classification of glaciers and advances our understanding of the seasonal velocity variations driven by multiple interacting processes.

5.1 Comparison between velocity simulation and observations

We compare the simulated velocity time series with velocities from satellite observations to determine whether seasonal velocity variations are influenced primarily by terminus change, co-influenced by subglacial hydrological system, or entirely independent of terminus change. We find that the velocity observations are well-described by the terminus-driven model for KUJ and EQP (Figures 2-3) but not for KAN and AVA (Figures 4-5). This indicates that both EQP and KUJ have type-1 velocity behavior. This is supported by the coincident timing of the end of terminus retreat and the peak summertime velocity (vertical black lines in Figures 2 and 3), even in instances when retreat continues beyond the end of the melt season (Figure 2). This is also supported by the percent difference between the simulated and observed velocities over all years, which are 5.0% for KUJ and 6.2% for EQP (Table S1), with correlations of 0.73 and 0.67, respectively (Figure 6) and low residuals (Figures 2 and 3). The stress coupling lengths chosen based on minimizing the difference between observed and modeled velocity are EQP = 10 km, KUJ = 20 km, KAN = 25 km, and AVA = 25 km (Table S1). However, KAN and AVA's seasonal velocities are not primarily driven by terminus variation, so we do not consider the estimation of stress coupling length valid for these glaciers.

For AVA and KAN, we find that simulated velocities differ substantially from the observed velocities suggesting that the terminus-driven model is insufficient to explain the observed velocities and that velocity change is not primarily driven by terminus fluctuations. For AVA, we find a poor correlation between observed and simulated velocity (-0.41; Figure 6) and residuals are just slightly smaller than the velocity observations themselves suggesting that the terminus-driven model can only explain ~37% of the observed velocity change. For KAN, the simulated and observed velocities are out of phase but of similar magnitude, producing small residuals (Figure 4) but a poor correlation, R=0.35 (Figure 6). Although our simulation results indicate no significant correlation between seasonal-scale glacier velocity changes and terminus variations at KAN, Kane et al. (2020) found a large, full-thickness calving event induced speed up in the frontal region of KAN on an hourly time-scale.

5.2 Non-terminus velocity processes

Although the terminus-driven model adequately resolves the majority of seasonal velocity variability for KUJ and EQP, the velocity residuals reveal additional sub-seasonal velocity changes that are not related to terminus change. One such signal is an additional pulse in velocity (acceleration and deceleration) that occurs near the middle of the melt season for all glaciers (Figures 2-5), meaning that all glaciers have type-2 behaivor. However, Vijay et al. (2021) claims that only AVA exhibited type-2 behavior in 2018. For KUJ, these melt-season pulses are not evident in the original velocity time series, but only become apparent in the velocity residuals, which further validates the effectiveness of our method in decomposing the coupled seasonal velocity variations of glaciers. We find that these mid-summer residual speed ups account for more than 80% of the observed





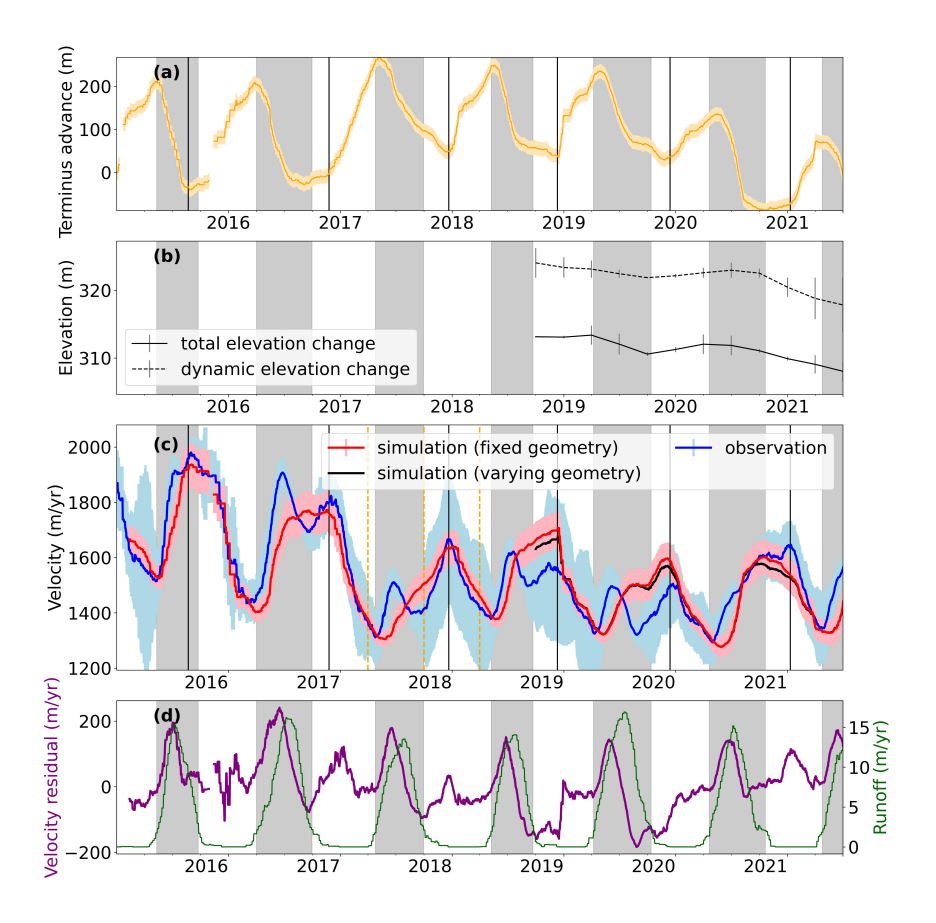


Figure 2. Time series for EQP. (a) Terminus position change time series from AutoTerm, with light yellow shading shows uncertainty. (b) Surface elevation from ICESat-2 data fusion. The dynamic elevation change is calculated by subtracting elevation change due to surface mass balance from total elevation change. (c) Observed and simulated velocity. Light blue and pink shading show the uncertainties of observations and simulations, respectively. (d) Velocity residual between observed and simulated velocity, along with the daily runoff from GSFC-FDMv1.2.1. The gray shaded vertical bars in all panes indicate when runoff is larger than 2 m/yr. The vertical black lines mark the onset of annual glacier retreat. The orange dashed lines in (c) marks the two periods in Figure 10a and b, respectively.

summertime velocity signal across all glaciers, with KAN and AVA exhibiting a higher percentage (91% and 86% respectively) than EQP and KUJ (84% and 82% respectively). We typically observe a lag time between the peak of the velocity residual followed by the peak of summer runoff (Figures 2-5). We conduct cross correlation analysis between the velocity residual and runoff to assess the time lag between the two and quantify the maximum correlation coefficient, thereby investigating the extent to which velocity is influenced by runoff. These lag times differ among glaciers, measuring 24 days for KUJ, 22 days for EQP, 47 days for KAN, and 51 days for AVA. The maximum correlation coefficients are 0.49 for KUJ, 0.73 for EQP, 0.67 for KAN, and 0.67 for AVA (Figure 7).





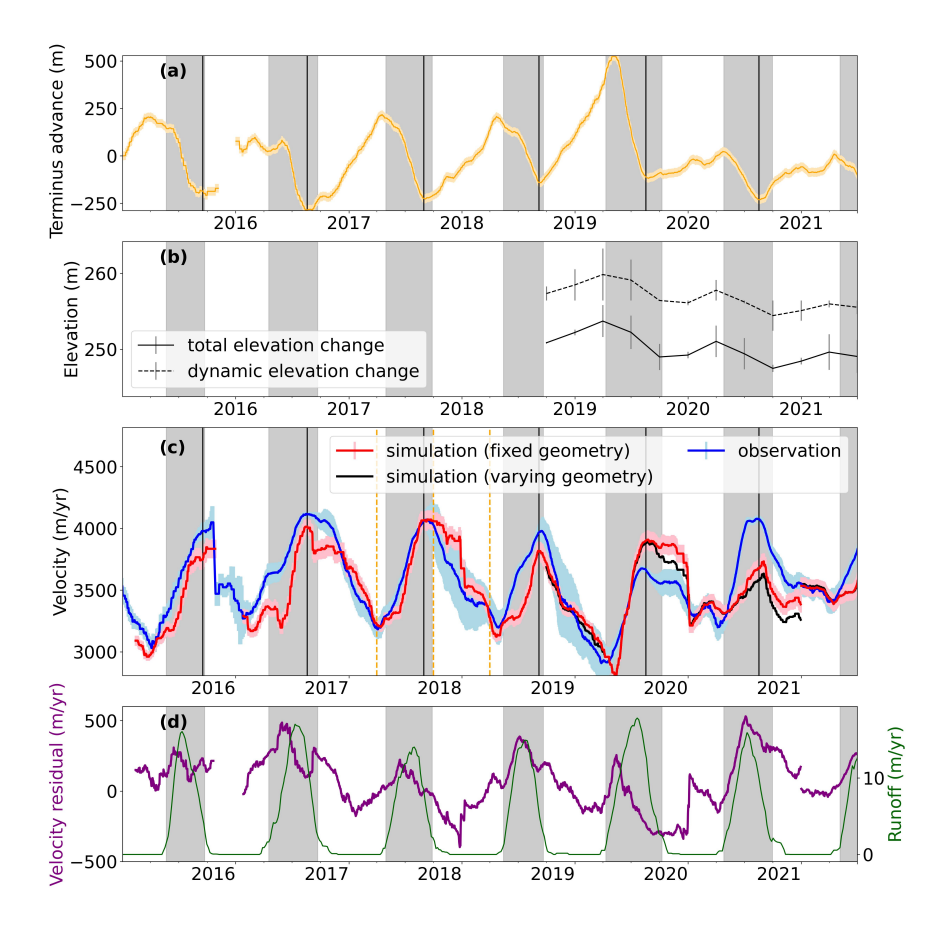


Figure 3. Time series for KUJ. The figure follows the same design as Figure 2. The orange dashed lines in (c) marks the two periods in Figure 10c and d,respectively.

For KAN and AVA, we observe accelerations during winter (during terminus advance) that plateau before the onset of the melt season in the following year, and early melt season accelerations with the annual maximum velocity reached in the middle of the melt season (Figures 4 and 5). This observation indicate that KAN and AVA has type-3 behavior, which is consistent with the classification of Vijay et al. (2021). The terminus-driven model does not capture wintertime acceleration because across all glaciers the terminus is advancing in winter. For KAN, the model predicts slight deceleration in winter (Figure 4). For AVA, there is no significant seasonality in the simulated velocity likely because the scale of seasonal terminus advance and retreat for this glacier is small (Figure 5) and the surface elevation is flat in frontal region. For reference the averaged seasonal range in terminus position is 144 meters for AVA, while EQP is 224 meters, KAN is 390 meters, and KUJ is 417 meters.





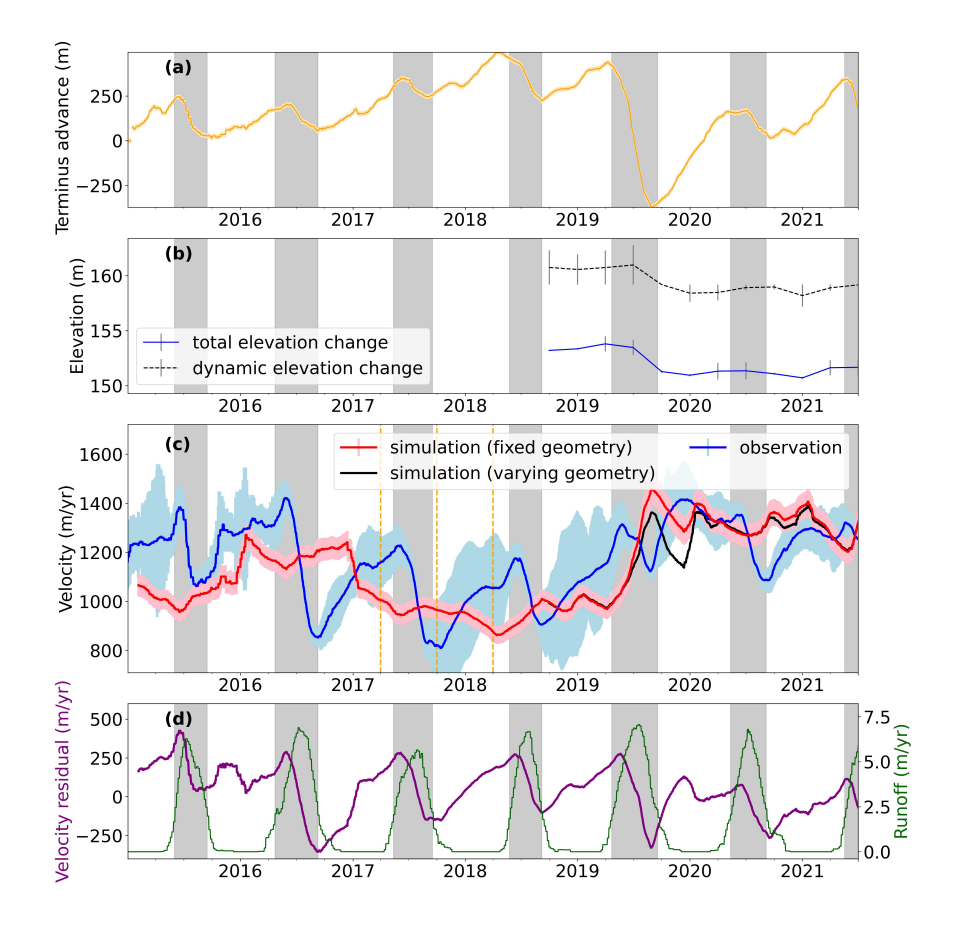


Figure 4. The full record of KAN. The figure follows the same design as Figure 2. The orange dashed lines in (c) marks the two periods in Figure 10e and f,respectively.

255 5.3 Experiments with seasonally varying surface elevation

We investigate the influence of changing surface topography by comparing the velocity simulated using a fixed geometry against the velocity simulated using a seasonally varying surface elevation from 2018-2022. We find minimal differences between these results for all glaciers (black versus red lines in Figures 2–5). Using KUJ as an example, the results from two analytical experiments involving artificially modified elevation profiles suggest that terminus-driven velocities are relatively insensitive to spatially uniform along-flow changes in surface elevation. In contrast, they show a high sensitivity to changes in surface slope (Figure 9). This result is important for providing context for interpreting the results of this model and our assumptions.





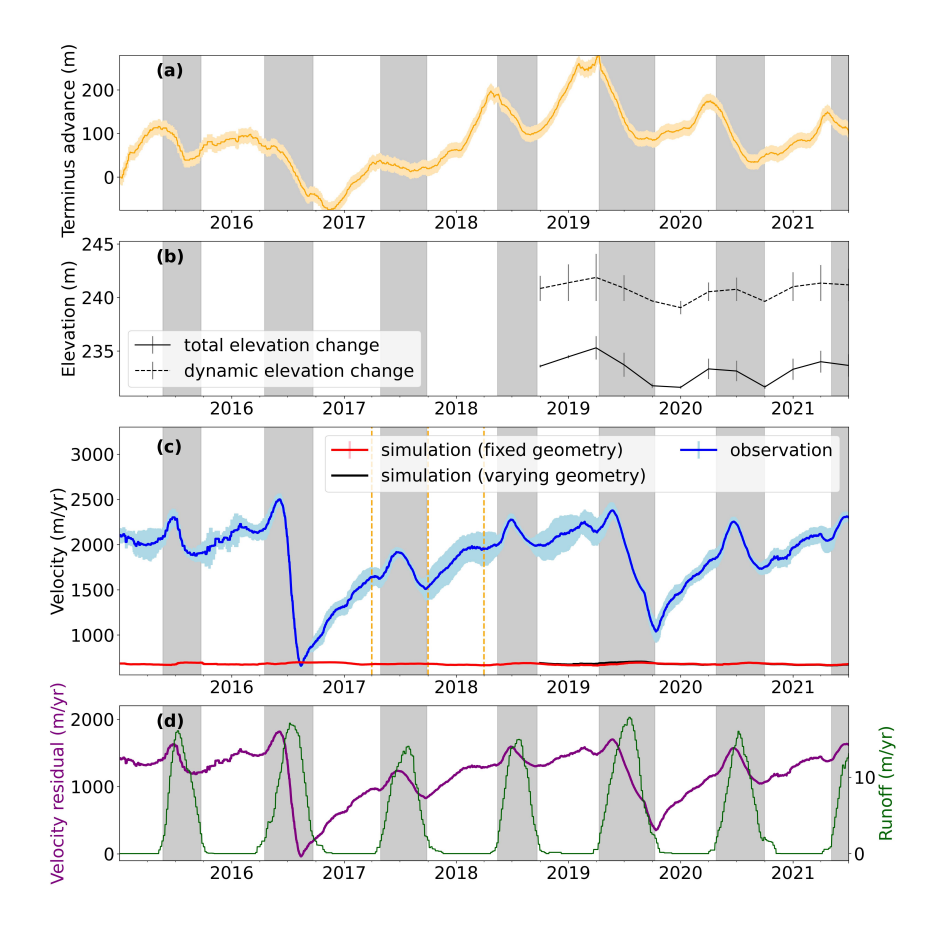


Figure 5. Time series for AVA. The figure follows the same design as Figure 2. The orange dashed lines in (c) marks the two periods in Figure 10g and h,respectively.

6 Discussion

Using observations with high temporal resolution and a terminus-driven model to simulate velocity variations resulting solely from terminus change, we investigate the controls on sub-seasonal velocity changes for four GrIS outlet glaciers and find that in all cases, glacier velocity responds to multiple compounding processes. The seasonal velocity changes of two glaciers (KUJ and EQP) can be largely attributed to seasonal terminus variation. All study glaciers experience sub-seasonal peaks in velocity that occur in the middle of the melt season and, AVA and KAN exhibit wintertime speedup that occurs when their termini are advancing (Figures 4 and 5).

We hypothesize that the peaks in velocity residuals observed for all glaciers during the middle of the melt season (Figures 2-5) are the result of meltwater-driven acceleration and subsequent evolution of the subglacial drainage system (Moon et al., 2014; Vijay et al., 2019). Early in the melt season, the subglacial drainage system is not fully channelized (Andrews et al., 2014),



280



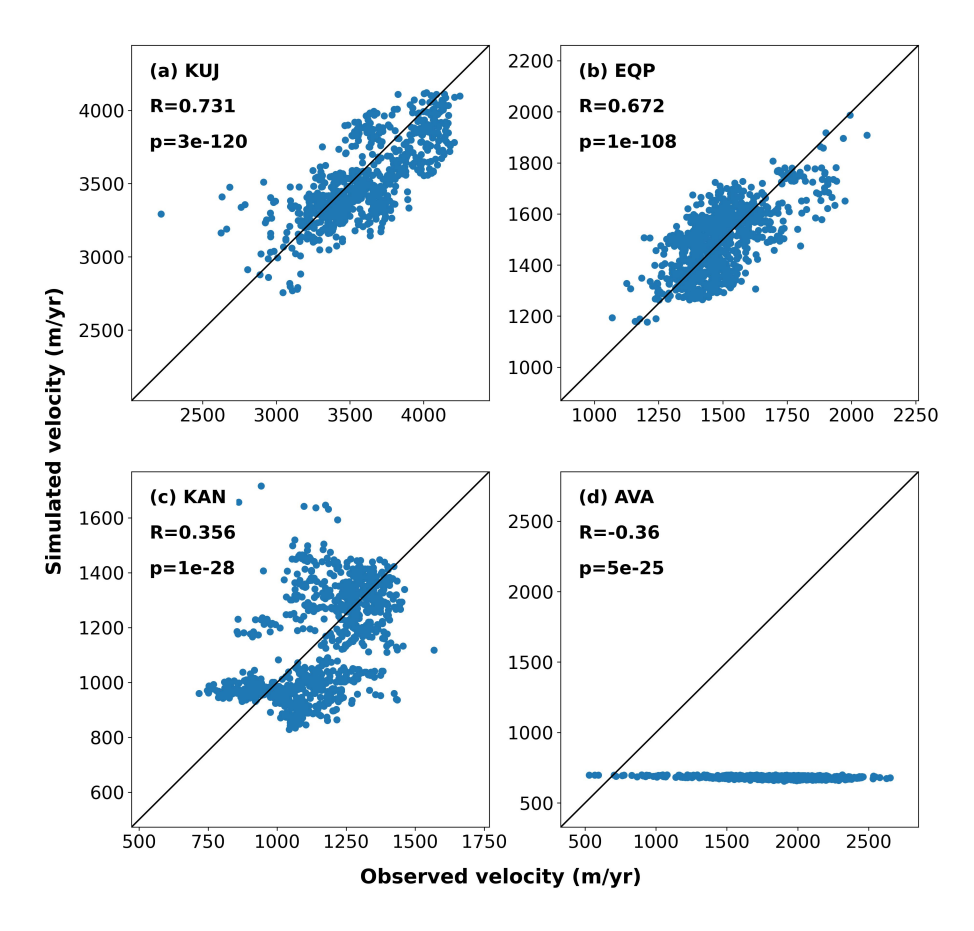


Figure 6. Scatter plot showing the comparison between simulated and observed velocity for KUJ, EQP, KAN, and AVA. The 1:1 line is as shown for each.

thus as meltwater availability begins to increase (marked by increasing runoff in early summer), subglacial water pressures increase, enhancing basal sliding by reducing friction between the ice and the bed (Bartholomew et al., 2010; Bartholomaus et al., 2008; Andrews et al., 2014). As the melt season progresses, the drainage system becomes more channelized, allowing for more efficient water drainage (Andrews et al., 2014; Schoof, 2010). Consequently, the available meltwater decreases, producing a reduction in glacier speed. This change in efficiency of the subglacial drainage system may explain the lag between peak velocity residual and peak runoff as has been shown by previous authors (King et al., 2020). The more readily the subglacial drainage system channelizes, the earlier the peak velocity residual occurs relative to peak runoff. Beyond the melt season, the impact of terminus retreat on seasonal velocities can become more pronounced. For example, EQP typically has a melt season that ends in October, but the terminus continues to retreat until December/January (the vertical black lines are usually behind the end of the gray bar in the same year in Figure 2). This produces a wintertime velocity peak that is coincident with the most retreated terminus of EQP and is distinct from the melt-season peak.



295



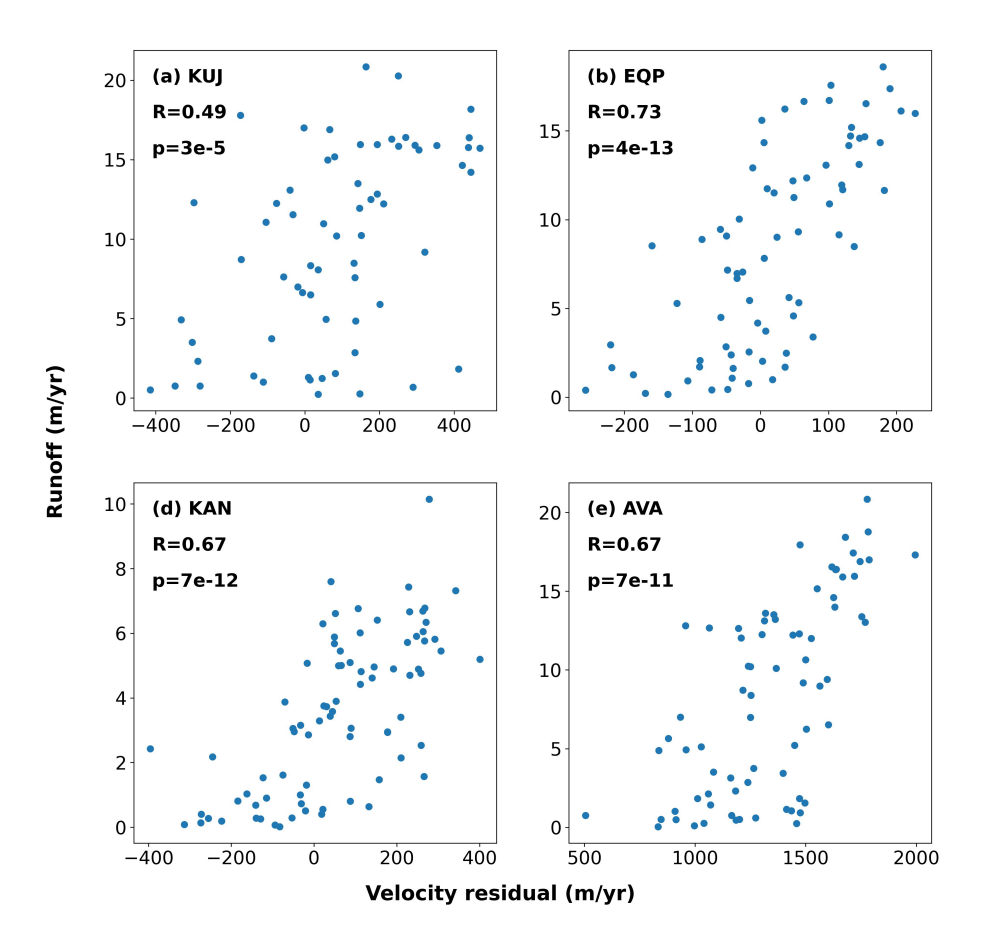


Figure 7. Scatter plot showing the comparison between velocity residual and runoff for KUJ, EQP, KAN, and AVA. The phases of velocity residual have been adjusted to achieve the maximum correlation coefficient.

To further explore the velocity increases that occur in summer, we examine the along-flow variability in velocity to determine how far upstream velocity changes occur (Figure 10). Our hypothesis is that changes in basal lubrication will be widespread over the region where water enters the bed, but downstream of the equilibrium line (Catania et al., 2017). To confirm that runoff drives the summertime speed up, we compare the along-flow spatial pattern of velocity change that occurs in the summer melt season of 2017 for EQP where summer velocity peaks are strongest (Apr 2017 - Sep 2017; Figure 10a) and the subsequent time period when runoff is low and the velocity is primarily influenced by terminus changes (Oct 2017 - Mar 2018; Figure 10b). The idea is that runoff-driven expansion of the subglacial drainage system would produce velocity changes that extend far inland from the terminus, while terminus-driven increases in velocity would decay rapidly from the terminus (Smith et al., 2017). The rapid decline in speed with distance from the terminus is expected when a glacier is terminus-driven because of the reduction in the terminus force with distance from the terminus (Joughin et al., 2012). Conversely, elevated inland velocities are typical for melt-driven acceleration (Sundal et al., 2011) because meltwater percolates throughout a large portion of the ablation zone (Andrews et al., 2014), which extends about 70 km inland of the terminus for EQP (Noël et al., 2019).



305



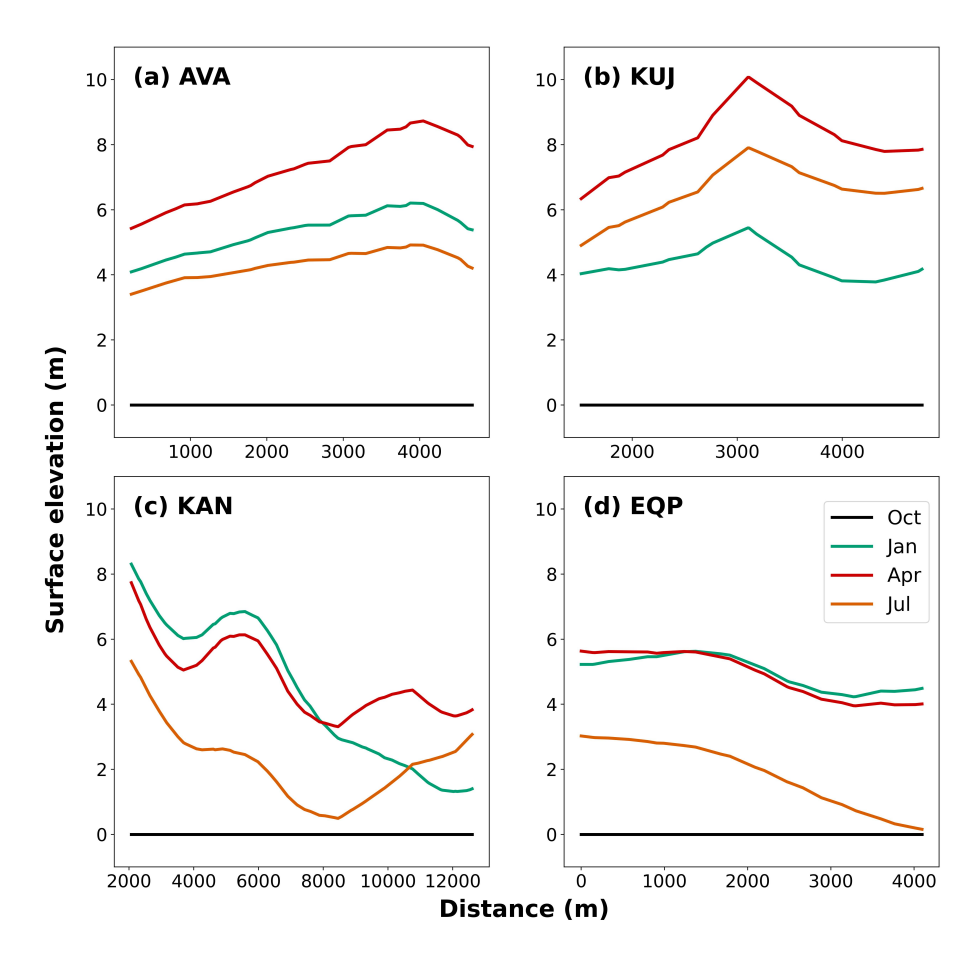


Figure 8. Surface elevation difference profiles for AVA, KUJ, KAN, and EQP in 2019 relative to the October profile.

We choose a distance of 10 km upstream from the terminus to represent the inland distance and compare the range in velocity in this location to the range in velocity found at a location that is 2 km from the terminus. A larger ratio of velocity range between the upstream and the frontal region, in conjunction with the correlation between velocity residuals and runoff data, indicate that the velocity is likely driven by runoff. For EQP, we find that in the summer (Apr-Sep) the upstream velocity range is 64% of that observed at the terminus (Figure 10a) while in winter (Oct-Mar) the upstream velocity is just 12% of what is observed at the terminus (Figure 10b). In addition to EQP, we also find that in summer (Apr-Sep) the upstream velocity ranges for both KAN and AVA are both 56% of that observed at the terminus (Figures 10e and g). Thus, we conclude that summer accelerations of EQP, KAN, and AVA is strongly caused by runoff, as it is more noticeable upstream compared to the velocity changes in EQP during the winter, which is driven by terminus changes. For KUJ, the ratio of velocity range between upstream and frontal region is 13% in summer (Apr-Sep) (Figure 10c), slightly larger than the 10% ratio observed in winter (Oct-Mar) (Figure 10d). Based on this observation, along with the correlation between KUJ's velocity residual and runoff



315

320

325



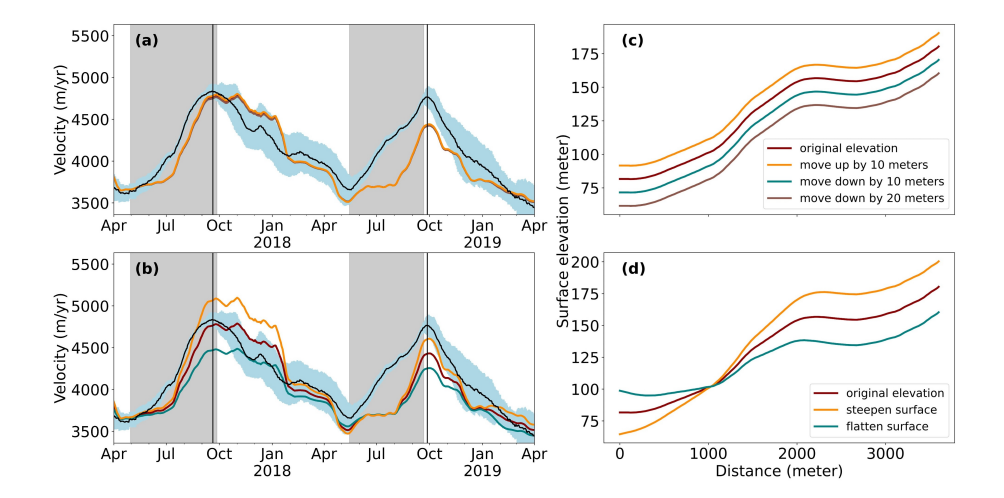


Figure 9. Experiment results using the artificially modified surface elevations. The results of (a) correspond to (c), and the results of (b) correspond to (d).

(Figure 7a), we conclude that runoff also influences the velocity changes of the KUJ glacier during the summer, although its impact is not as pronounced as that on the other three glaciers.

While AVA and KAN experience mid-summer velocity pulses similar to EQP, they do not exhibit any terminus-driven seasonal acceleration (Figures 4 and 5) and instead accelerate in winter. This is suggested by the poor correlation between velocity changes and terminus changes for these glaciers. We examine wintertime acceleration similar to above by determining the along-flow pattern of velocity change (Figure 10f and h). For both glaciers we find significant inland acceleration in winter. For KAN, the range in upstream velocity during winter is 72% of the range in frontal velocity and for AVA, the range in upstream velocity is 36% of the range of frontal velocity, which is larger than terminus-driven upstream velocity range that was observed for EQP (Figures 10f and h versus b). We hypothesize that the elevated range of KAN and AVA's upstream velocities in winter suggests that winter acceleration is due to enhanced extensive basal slip. For many parts of Greenland, basal water is generated year-round because of friction at the ice-bed interface and geothermal heat (Karlsson et al., 2021). During the onset of winter, refreezing of available basal water (Boon and Sharp, 2003) and viscous deformation over subglacial conduits (Vieli et al., 2004; Bartholomaus et al., 2011) can obstruct the drainage system. Consequently, water becomes trapped within an inefficient drainage network, leading to increased water pressure and winter acceleration (Vijay et al., 2019). The winter acceleration phase ends when the melt season begins to supply significant volumes of additional water to the subglacial system, which increases basal water pressures causing summertime acceleration (Davison et al., 2020).

Our examination of how our model performs further upstream of the terminus (Supplementary Information) informs the transmission distances for terminus perturbations. Enderlin et al. (2016) estimates the stress coupling length using an empirical method, suggesting that the stress coupling length should be approximately four times the glacier thickness, which produces values of 752 m for EQP and 2236 m for KUJ. These values are much smaller than our estimated stress coupling length



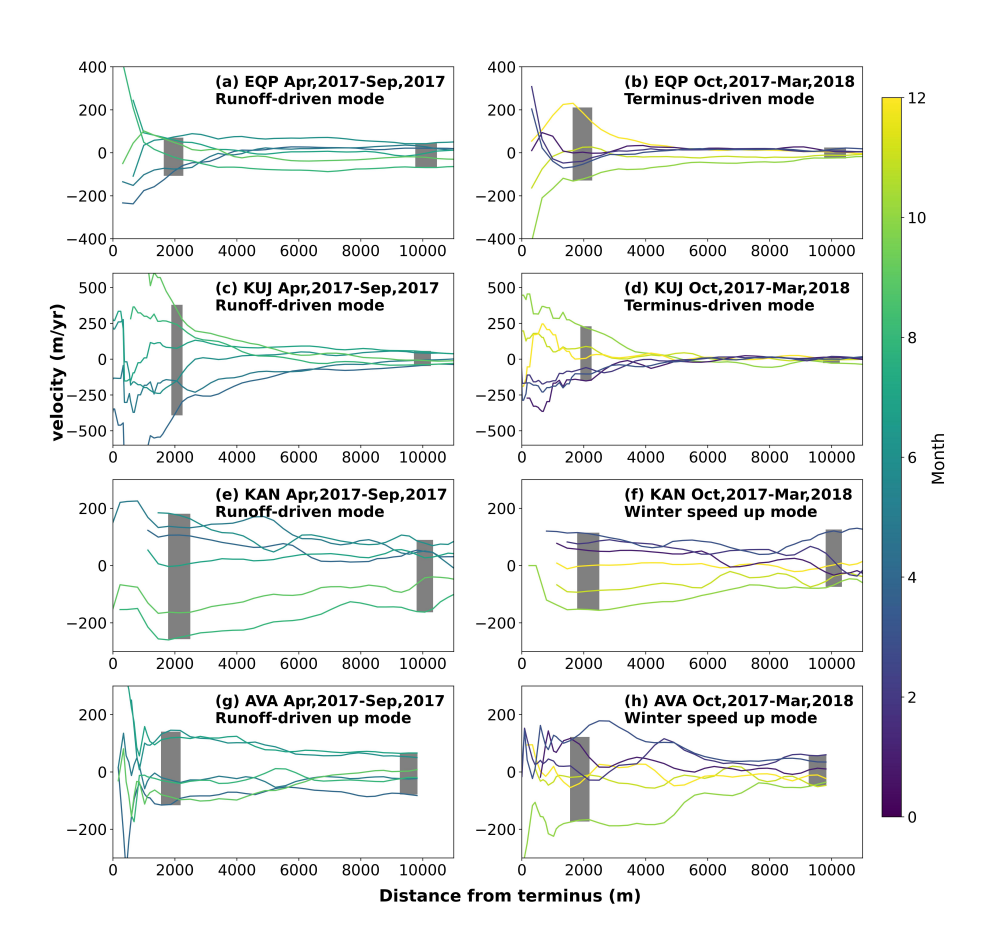


Figure 10. Velocity profiles over time for EQP, KUJ, KAN, and AVA. The average velocity profile has been subtracted for a better display of changes over time. The original velocity profiles are shown in Figure S8. The shaded areas indicate regions where we obtain velocity variations in the frontal and upstream sections. (a) Velocity profiles of EQP during the melt season. (b) Velocity profiles of EQP after the melt season, during which velocity is primarily influenced by terminus changes. (c) Velocity profiles of KUJ during the melt season. (d) Velocity profiles of KUJ after the melt season. (e) Velocity profile of KAN during melt season. (f) Velocity profile of KAN after the melt season.



330

335

340

345

350

355



based on minimizing the difference between observed and modeled velocity (EQP = 10 km and KUJ = 20 km; Table S1) suggesting that changes at the terminus might translate much farther upstream for those glaciers that have seasonal velocity changes largely driven by terminus change. This aligns with results from (Felikson et al., 2017), who use an analysis of the Peclet number for these glaciers to determine how far inland terminus perturbations can diffuse. They found that terminus perturbations can diffuse inland to 15 km for EQP and 27 km for KUJ.

6.1 Impact of observed seasonal elevation changes

The availability of seasonally-resolved elevation change allows us to investigate the degree to which outlet glacier terminus velocity is sensitive to changing surface elevation. We find that seasonal elevation changes for EQP, KAN, KUJ, and AVA are relatively uniform along flow in the frontal region (Figure 8). On average, within the initial 4000 meters of the elevation profile near the terminus, the standard deviation of elevation change is 12% of the mean elevation change along the profile. Thus, the seasonal elevation change is largely uniform across the DEM and these elevation changes do not significantly alter terminus-driven velocity (black lines in Figures 2–5). This aligns with our experimental results that suggest that vertical shifts in elevation have a limited contribution to velocity seasonality (Figure 9a) but that steepening the surface elevation will cause stronger velocity responses to terminus variations (Figure 9b).

7 Limitations and Outlook

We recognize that the choice of the terminus-driven model to explore how outlet glacier velocity might respond to terminus change is simplified over that from numerical results. There are several important limitations that merit further discussion. Seasonal elevation change is not yet available widely and may be important to include for some glaciers, particularly ones that are experiencing changes in slope near the terminus, which might influence ice velocity. The model only looks at the impact of terminus change on ice velocity and thus many important processes that control ice velocity are lumped into the examination of the velocity residuals. Here we have considered processes such as melt-driven changes in velocity and wintertime acceleration related to meltwater at the bed. However, other factors such as sea ice/melange and air temperatures (Walter et al., 2012; Carr et al., 2013) could also influence a glacier's seasonal and inter-annual variations, warranting further investigation.

In addition to these limitations, the model only captures longitudinal stresses, not lateral stresses. Since floating ice can experience velocity variations that are driven by nearby velocities on the grounded ice through transmission of lateral stress, the model is not appropriate for use on floating ice. The terminus-driven model importantly only applies close to the terminus since by definition, the frontal force F linearly decreases upstream of the terminus to zero at the stress coupling length.

Despite these shortcomings, the terminus-driven model provides a means to isolate the impact of seasonal terminus variations on outlet glacier velocity without numerical methods. Thus, it provides a quick assessment of outlet glacier terminus control and how this may change with time. Future work could examine how seasonal controls on ice velocity might vary from glacier to glacier and how those seasonal controls change during periods when glaciers are experiencing year over year terminus





retreat. Further, the terminus-driven model is useful for illustrating the multiple processes that act in concert to drive glacier velocity changes suggesting that simple categorization of glacier velocities as the result of a single process are not correct.

8 Conclusions

360

365

370

380

We apply a terminus-driven model to elucidate the degree to which seasonal terminus change can explain seasonal velocity variations for four glaciers in Central West Greenland. The comparison between simulated and observed velocity suggests that all glaciers experience multiple drivers of velocity change. Some glaciers experience seasonal velocity changes that are dominated by terminus change and some glaciers do not respond to terminus change because either the terminus change is too small to be impactful and/or other processes dominate velocity, notably wintertime acceleration. Importantly, velocity residuals allow for us to see that runoff-driven acceleration occurs for all glaciers but its impact is limited to the early melt season. We present a new fusion of elevation products that resolve seasonal elevation changes for our study glaciers. When integrated into our model we do not find a significant difference between simulated velocities driven by terminus change assuming a fixed surface elevation versus those with an evolving surface elevation. We show that this is because the observed seasonal elevation change is largely the result of a vertical shift in surface elevation with no noticeable slope change, which would drive a velocity response. Our study highlights how a simple model can be used to examine the impact of terminus change on near-terminus velocity and allows a method for distinguishing the controls on seasonal velocity change of outlet glaciers. Moreover, the same framework could be applied to investigate the long-term changes in glacier dynamics with adequate historical data.

Code and data availability. Velocity time series data are available at Gardner et al. (2023). Velocity monthly mosaics are available at Joughin (2023). ArcticDEMs are available at Porter et al. (2022). BedMachineV5 is available at Morlighem et al. (2022). QGreenland package is available at Moon et al. (2023). The code, terminus data, flowlines, and DG-IS2-DEMs on which this article is based are available at Zhang (2023).

Author contributions. EZ developed the code, performed the data processing, and wrote the manuscript. BS developed "DG-IS2-DEM". GC, DF, BC, and DT advised EZ and revised the manuscript.

Competing interests. One of the co-authors is in the editorial board of The Cryosphere.

Acknowledgements. We acknowledge funding for this work from NASA (Grant NNH20ZDA001N-ICESAT2) and the Institute for Geophysics Postdoctoral Fellowship at the Jackson School to E. Zhang. We acknowledge the National Snow and Ice Data Center QGreenland





package (Moon et al., 2023). We acknowledge DEMs provided by the Polar Geospatial Center under NSF-OPP awards 1043681, 1559691, 1542736, 1810976, and 2129685.





385 References

395

405

- An, L., Rignot, E., Mouginot, J., and Millan, R.: A Century of Stability of Avannarleq and Kujalleq Glaciers, West Greenland, Explained Using High-Resolution Airborne Gravity and Other Data, Geophysical Research Letters, 45, 3156–3163, https://doi.org/10.1002/2018GL077204, 2018.
- Andrews, L. C., Catania, G. A., Hoffman, M. J., Gulley, J. D., Lüthi, M. P., Ryser, C., Hawley, R. L., and Neumann, T. A.: Direct observations of evolving subglacial drainage beneath the Greenland Ice Sheet, Nature, 514, 80–83, https://doi.org/10.1038/nature13796, 2014.
 - Bartholomaus, T. C., Anderson, R. S., and Anderson, S. P.: Response of glacier basal motion to transient water storage, Nature Geoscience, 1, 33–37, https://doi.org/10.1038/ngeo.2007.52, 2008.
 - Bartholomaus, T. C., Anderson, R. S., and Anderson, S. P.: Growth and collapse of the distributed subglacial hydrologic system of Kennicott Glacier, Alaska, USA, and its effects on basal motion, Journal of Glaciology, 57, 985–1002, https://doi.org/10.3189/002214311798843269, 2011.
 - Bartholomew, I., Nienow, P., Mair, D., Hubbard, A., King, M. A., and Sole, A.: Seasonal evolution of subglacial drainage and acceleration in a Greenland outlet glacier, Nature Geoscience, 3, 408–411, https://doi.org/10.1038/ngeo863, 2010.
 - Black, T. E. and Joughin, I.: Weekly to monthly terminus variability of Greenland's marine-terminating outlet glaciers, The Cryosphere, 17, 1–13, https://doi.org/10.5194/tc-17-1-2023, 2023.
- Boon, S. and Sharp, M.: The role of hydrologically-driven ice fracture in drainage system evolution on an Arctic glacier, Geophysical Research Letters, 30, https://doi.org/https://doi.org/10.1029/2003GL018034, 2003.
 - Bézu, C. and Bartholomaus, T. C.: Greenland Ice Sheet's Distinct Calving Styles Are Identified in Terminus Change Timeseries, Geophysical Research Letters, 51, https://doi.org/10.1029/2024gl110224, 2024.
 - Carnahan, E., Catania, G., and Bartholomaus, T. C.: Observed mechanism for sustained glacier retreat and acceleration in response to ocean warming around Greenland, The Cryosphere, 16, 4305–4317, https://doi.org/10.5194/tc-16-4305-2022, 2022.
 - Carr, J. R., Vieli, A., and Stokes, C.: Influence of sea ice decline, atmospheric warming, and glacier width on marine-terminating outlet glacier behavior in northwest Greenland at seasonal to interannual timescales, Journal of Geophysical Research: Earth Surface, 118, 1210–1226, https://doi.org/10.1002/jgrf.20088, 2013.
- Catania, G. A., Neumann, T. A., and Price, S. F.: Characterizing englacial drainage in the ablation zone of the Greenland ice sheet, Journal of Glaciology, 54, 567–578, https://doi.org/10.3189/002214308786570854, 2017.
 - Catania, G. A., Stearns, L. A., Sutherland, D. A., Fried, M. J., Bartholomaus, T. C., Morlighem, M., Shroyer, E., and Nash, J.: Geometric controls on tidewater glacier retreat in central western Greenland, Journal of Geophysical Research: Earth Surface, 123, 2024–2038, https://doi.org/10.1029/2017JF004499, 2018.
- Davison, B. J., Sole, A. J., Cowton, T. R., Lea, J. M., Slater, D. A., Fahrner, D., and Nienow, P. W.: Subglacial Drainage Evolution Modulates

 Seasonal Ice Flow Variability of Three Tidewater Glaciers in Southwest Greenland, Journal of Geophysical Research: Earth Surface, 125, e2019JF005 492, https://doi.org/https://doi.org/10.1029/2019JF005492, 2020.
 - Enderlin, E. M., Howat, I. M., Jeong, S., Noh, M.-J., van Angelen, J. H., and van den Broeke, M. R.: An improved mass budget for the Greenland ice sheet, Geophysical Research Letters, 41, 866–872, https://doi.org/10.1002/2013GL059010, 2014.
- Enderlin, E. M., Hamilton, G. S., O'Neel, S., Bartholomaus, T. C., Morlighem, M., and Holt, J. W.: An empirical approach for estimating stress-coupling lengths for marine-terminating glaciers, Frontiers in Earth Science, 4, 104, https://doi.org/10.3389/feart.2016.00104, 2016.





- Felikson, D., Bartholomaus, T. C., Catania, G. A., Korsgaard, N. J., Kjær, K. H., Morlighem, M., Noël, B., Van Den Broeke, M., Stearns, L. A., Shroyer, E. L., et al.: Inland thinning on the Greenland ice sheet controlled by outlet glacier geometry, Nature Geoscience, 10, 366–369, https://doi.org/10.1038/ngeo2934, 2017.
- Felikson, D., A. Catania, G., Bartholomaus, T. C., Morlighem, M., and Noël, B. P. Y.: Steep Glacier Bed Knickpoints Mitigate Inland Thinning in Greenland, Geophysical Research Letters, 48, e2020GL090112, https://doi.org/10.1029/2020GL090112, 2021.
 - Felikson, D., Nowicki, S., Nias, I., Morlighem, M., and Seroussi, H.: Seasonal Tidewater Glacier Terminus Oscillations Bias Multi-Decadal Projections of Ice Mass Change, Journal of Geophysical Research: Earth Surface, 127, e2021JF006249, https://doi.org/https://doi.org/10.1029/2021JF006249, 2022.
- Fried, M. J., Catania, G. A., Stearns, L. A., Sutherland, D. A., Bartholomaus, T. C., Shroyer, E., and Nash, J.: Reconciling Drivers of Seasonal
 Terminus Advance and Retreat at 13 Central West Greenland Tidewater Glaciers, Journal of Geophysical Research: Earth Surface, 123,
 1590–1607, https://doi.org/10.1029/2018JF004628, 2018.
 - Gardner, A. S., Moholdt, G., Scambos, T., Fahnstock, M., Ligtenberg, S., van den Broeke, M., and Nilsson, J.: Increased West Antarctic and unchanged East Antarctic ice discharge over the last 7 years, The Cryosphere, 12, 521–547, https://doi.org/10.5194/tc-12-521-2018, 2018.
- Gardner, A. S., Fahnestock, M. A., and Scambos, T. A.: ITS_LIVE Regional Glacier and Ice Sheet Surface Velocities (Version 1), https://doi: 10.5067/6II6VW8LLWJ7, 2023.
 - Goliber, S. A. and Catania, G. A.: Glacier Terminus Morphology Informs Calving Style, Geophysical Research Letters, 51, https://doi.org/10.1029/2024gl108530, 2024.
 - Holland, D. M., Thomas, R. H., De Young, B., Ribergaard, M. H., and Lyberth, B.: Acceleration of Jakobshavn Isbræ triggered by warm subsurface ocean waters, Nature geoscience, 1, 659–664, https://doi.org/10.1038/ngeo316, 2008.
- Howat, I. M., Joughin, I., Tulaczyk, S., and Gogineni, S.: Rapid retreat and acceleration of Helheim Glacier, east Greenland, Geophysical Research Letters, 32, L22 502, https://doi.org/10.1029/2005GL024737, 2005.
 - Howat, I. M., Joughin, I., Fahnestock, M., Smith, B. E., and Scambos, T. A.: Synchronous retreat and acceleration of southeast Greenland outlet glaciers 2000–06: ice dynamics and coupling to climate, Journal of Glaciology, 54, 646–660, https://doi.org/10.3189/002214308786570908, 2008.
- 445 IPCC: Climate Change 2022: Mitigation of Climate Change, Cambridge University Press, Cambridge, UK and New York, NY, USA, https://doi.org/10.1017/9781009157926, 2022.
 - Joughin, I.: MEaSUREs Greenland Monthly Ice Sheet Velocity Mosaics from SAR and Landsat (Version 5), https://nsidc.org/data/ NSIDC-0731/versions/5, 2023.
- Joughin, I., Das, S. B., King, M. A., Smith, B. E., Howat, I. M., and Moon, T.: Seasonal speedup along the Western flank of the Greenland

 450 Ice Sheet, Science, 320, 781–783, https://doi.org/10.1126/science.1153288, 2008.
 - Joughin, I., Smith, B. E., Howat, I. M., Floricioiu, D., Alley, R. B., Truffer, M., and Fahnestock, M.: Seasonal to decadal scale variations in the surface velocity of Jakobshavn Isbrae, Greenland: Observation and model-based analysis, Journal of Geophysical Research: Earth Surface, 117, F02 030, https://doi.org/10.1029/2011JF002110, 2012.
- Kane, E., Rignot, E., Mouginot, J., Millan, R., Li, X., Scheuchl, B., and Fahnestock, M.: Impact of Calving Dynamics on Kangilernata Sermia, Greenland, Geophysical Research Letters, 47, e2020GL088 524, https://doi.org/https://doi.org/10.1029/2020GL088524, 2020.
 - Karlsson, N. B., Solgaard, A. M., Mankoff, K. D., Gillet-Chaulet, F., MacGregor, J. A., Box, J. E., Citterio, M., Colgan, W. T., Larsen, S. H., Kjeldsen, K. K., Korsgaard, N. J., Benn, D. I., Hewitt, I. J., and Fausto, R. S.: A first constraint on basal melt-water production of the Greenland ice sheet, Nature Communications, 12, 3461, https://doi.org/10.1038/s41467-021-23739-z, 2021.





- King, M. D., Howat, I. M., Jeong, S., Noh, M. J., Wouters, B., Noël, B., and van den Broeke, M. R.: Seasonal to decadal variability in ice discharge from the Greenland Ice Sheet, The Cryosphere, 12, 3813–3825, https://doi.org/10.5194/tc-12-3813-2018, 2018.
 - King, M. D., Howat, I. M., Candela, S. G., Noh, M. J., Jeong, S., Noël, B. P., van den Broeke, M. R., Wouters, B., and Negrete, A.: Dynamic ice loss from the Greenland Ice Sheet driven by sustained glacier retreat, Communications Earth & Environment, 1, 1, https://doi.org/10.1038/s43247-020-0001-2, 2020.
- Kneib-Walter, A., Lüthi, M. P., Moreau, L., and Vieli, A.: Drivers of Recurring Seasonal Cycle of Glacier Calving Styles and Patterns,

 Frontiers in Earth Science, 9, https://doi.org/10.3389/feart.2021.667717, 2021.
 - Kneib-Walter, A., Lüthi, M. P., Funk, M., Jouvet, G., and Vieli, A.: Observational constraints on the sensitivity of two calving glaciers to external forcings, Journal of Glaciology, 69, 459–474, https://doi.org/10.1017/jog.2022.74, 2023.
 - LÜTHI, M. P., VIELI, A., MOREAU, L., JOUGHIN, I., REISSER, M., SMALL, D., and STOBER, M.: A century of geometry and velocity evolution at Eqip Sermia, West Greenland, Journal of Glaciology, 62, 640–654, https://doi.org/10.1017/jog.2016.38, 2016.
- Medley, B., Neumann, T. A., Zwally, H. J., Smith, B. E., and Stevens, C. M.: Simulations of firn processes over the Greenland and Antarctic ice sheets: 1980–2021, The Cryosphere, 16, 3971–4011, https://doi.org/10.5194/tc-16-3971-2022, 2022.
 - Moon, T., Joughin, I., Smith, B., and Howat, I.: 21st-Century evolution of Greenland outlet glacier velocities, Science, 336, 576–578, https://doi.org/10.1126/science.1219985, 2012.
- Moon, T., Joughin, I., Smith, B., van den Broeke, M. R., van de Berg, W. J., Noël, B., and Usher, M.: Distinct patterns of seasonal Greenland glacier velocity, Geophysical Research Letters, 41, 7209–7216, https://doi.org/10.1002/2014GL061836, 2014.
 - Moon, T., Joughin, I., and Smith, B.: Seasonal to multiyear variability of glacier surface velocity, terminus position, and sea ice/ice mélange in northwest Greenland, Journal of Geophysical Research: Earth Surface, 120, 818–833, https://doi.org/10.1002/2015JF003494, 2015.
 - Moon, T., Gardner, A., Csatho, B., Parmuzin, I., and Fahnestock, M.: Rapid reconfiguration of the Greenland Ice Sheet coastal margin, Journal of Geophysical Research: Earth Surface, 125, https://doi.org/10.1029/2020jf005585, 2020.
- 480 Moon, T., Fisher, M., Stafford, T., and Thurber, A.: QGreenland (v3), National Snow and Ice Data Center, https://10.5281/zenodo.8326507, 2023.
 - Morlighem, M., Williams, C. N., Rignot, E., An, L., Arndt, J. E., Bamber, J. L., Catania, G., Chauché, N., Dowdeswell, J. A., Dorschel, B., Fenty, I., Hogan, K., Howat, I., Hubbard, A., Jakobsson, M., Jordan, T. M., Kjeldsen, K. K., Millan, R., Mayer, L., Mouginot, J., Noël, B. P. Y., O'Cofaigh, C., Palmer, S., Rysgaard, S., Seroussi, H., Siegert, M. J., Slabon, P., Straneo, F., van den Broeke,
- M. R., Weinrebe, W., Wood, M., and Zinglersen, K. B.: BedMachine v3: Complete bed topography and ocean bathymetry mapping of Greenland from multibeam echo dounding combined with mass conservation, Geophysical Research Letters, 44, 11,051–11,061, https://doi.org/10.1002/2017GL074954, 2017.
 - Morlighem, M., Williams, C. N., Rignot, E., An, L., Arndt, J. E., Bamber, J. L., Catania, G., Chauché, N., Dowdeswell, J. A., Dorschel, B., Fenty, I., Hogan, K., Howat, I., Hubbard, A., Jakobsson, M., Jordan, T. M., Kjeldsen, K. K., Millan, R., Mayer, L., Mouginot, J., Noël, B.
- 490 P. Y., O'Cofaigh, C., Palmer, S., Rysgaard, S., Seroussi, H., Siegert, M. J., Slabon, P., Straneo, F., van den Broeke, M. R., Weinrebe, W., Wood, M., and Zinglersen, K. B.: IceBridge BedMachine Greenland, Version 5, https://doi.org/10.5067/GMEVBWFLWA7X., 2022.
 - Noël, B., van de Berg, W. J., Lhermitte, S., and van den Broeke, M. R.: Rapid ablation zone expansion amplifies north Greenland mass loss, Science Advances, 5, eaaw0123, https://doi.org/10.1126/sciadv.aaw0123, 2019.
- Poinar, K.: Seasonal Flow Types of Glaciers in Sermilik Fjord, Greenland, Over 2016–2021, Journal of Geophysical Research: Earth Surface, 128, e2022JF006 901, https://doi.org/10.1029/2022JF006901, 2023.



520

530



- Porter, C., Morin, P., Howat, I. M., Noh, M.-J., Bates, B., Peterman, K., Keesey, S., Schlenk, M., Gardiner, J., Tomko, K., Willis, M. J., Kelleher, C., Cloutier, M., Husby, E., Foga, S., Nakamura, H., Platson, M., Wethington, M. J., Williamson, C. J., Bauer, G., Enos, J., Arnold, G., Kramer, W., Becker, P., Doshi, A., D'Souza, C., Cummens, P., Laurier, F., and Bojesen, M.: ArcticDEM Strips (Version 4.1), https://doi.org/10.7910/DVN/C98DVS, 2022.
- Robel, A. A., Roe, G. H., and Haseloff, M.: Response of marine-terminating glaciers to forcing: time scales, sensitivities, instabilities and stochastic dynamics, Journal of Geophysical Research: Earth Surface, pp. 1 62, https://doi.org/10.1029/2018jf004709, 2018.
 - Schoof, C. G.: Ice-sheet acceleration driven by melt supply variability., Nature, 468, 803 806, https://doi.org/10.1038/nature09618, 2010.
 - Sergienko, O. V.: Marine outlet glacier dynamics, steady states and steady-state stability, Journal of Glaciology, 68, 946–960, https://doi.org/10.1017/jog.2022.13, 2022.
- Shepherd, A., Ivins, E. R., A, G., Barletta, V. R., Bentley, M. J., Bettadpur, S., Briggs, K. H., Bromwich, D. H., Forsberg, R., Galin, N., Horwath, M., Jacobs, S., Joughin, I., King, M. A., Lenaerts, J. T. M., Li, J., Ligtenberg, S. R. M., Luckman, A., Luthcke, S. B., McMillan, M., Meister, R., Milne, G., Mouginot, J., Muir, A., Nicolas, J. P., Paden, J., Payne, A. J., Pritchard, H., Rignot, E., Rott, H., Sørensen, L. S., Scambos, T. A., Scheuchl, B., Schrama, E. J. O., Smith, B., Sundal, A. V., van Angelen, J. H., van de Berg, W. J., van den Broeke, M. R., Vaughan, D. G., Velicogna, I., Wahr, J., Whitehouse, P. L., Wingham, D. J., Yi, D., Young, D., and Zwally, H. J.: A reconciled estimate of ice-sheet mass balance, Science, 338, 1183–1189, https://doi.org/10.1126/science.1228102, 2012.
 - Smith, L. C., Yang, K., Pitcher, L. H., Overstreet, B. T., Chu, V. W., Åsa K. Rennermalm, Ryan, J. C., Cooper, M. G., Gleason, C. J., Tedesco, M., Jeyaratnam, J., van As, D., van den Broeke, M. R., van de Berg, W. J., Noël, B., Langen, P. L., Cullather, R. I., Zhao, B., Willis, M. J., Hubbard, A., Box, J. E., Jenner, B. A., and Behar, A. E.: Direct measurements of meltwater runoff on the Greenland ice sheet surface, Proceedings of the National Academy of Sciences, 114, E10 622–E10 631, https://doi.org/10.1073/pnas.1707743114, 2017.
- 515 Solgaard, A. M., Rapp, D., Noël, B. P. Y., and Hvidberg, C. S.: Seasonal Patterns of Greenland Ice Velocity From Sentinel-1 SAR Data Linked to Runoff, Geophysical Research Letters, 49, e2022GL100 343, https://doi.org/https://doi.org/10.1029/2022GL100343, 2022.
 - Stevens, L. A., Nettles, M., Davis, J. L., Creyts, T. T., Kingslake, J., Hewitt, I. J., and Stubblefield, A.: Tidewater-glacier response to supraglacial lake drainage, Nature Communications, 13, 6065, https://doi.org/10.1038/s41467-022-33763-2, 2022.
 - Sundal, A. V., Shepherd, A., Nienow, P., Hanna, E., Palmer, S., and Huybrechts, P.: Melt-induced speed-up of Greenland ice sheet offset by efficient subglacial drainage, Nature, 469, 521–524, https://doi.org/10.1038/nature09740, 2011.
 - Ultee, L., Felikson, D., Minchew, B., Stearns, L. A., and Riel, B.: Helheim Glacier ice velocity variability responds to runoff and terminus position change at different timescales, Nature Communications, 13, 6022, https://doi.org/10.1038/s41467-022-33292-y, 2022.
- van den Broeke, M. R., Enderlin, E. M., Howat, I. M., Kuipers Munneke, P., Noël, B. P. Y., van de Berg, W. J., van Meijgaard, E., and Wouters,
 B.: On the recent contribution of the Greenland ice sheet to sea level change, The Cryosphere, 10, 1933–1946, https://doi.org/10.5194/tc10-1933-2016, 2016.
 - van der Veen, C. J.: Fundamentals of glacier dynamics, CRC press, New York, second edition edn., 2013.
 - van der Veen, C. J., Plummer, J., and Stearns, L. A.: Controls on the recent speed-up of Jakobshavn Isbrae, West Greenland, Journal of Glaciology, 57, 770 782, 2011.
 - Vieli, A., Jania, J., Blatter, H., and Funk, M.: Short-term velocity variations on Hansbreen, a tidewater glacier in Spitsbergen, Journal of Glaciology, 50, 389–398, https://doi.org/10.3189/172756504781829963, 2004.
 - Vijay, S., Khan, S. A., Kusk, A., Solgaard, A. M., Moon, T., and Bjørk, A. A.: Resolving Seasonal Ice Velocity of 45 Greenlandic Glaciers With Very High Temporal Details, Geophysical Research Letters, 46, 1485–1495, https://doi.org/https://doi.org/10.1029/2018GL081503, 2019.





- Vijay, S., King, M. D., Howat, I. M., Solgaard, A. M., Khan, S. A., and Noël, B.: Greenland ice-sheet wide glacier classification based on two distinct seasonal ice velocity behaviors, Journal of Glaciology, 67, 1241–1248, https://doi.org/10.1017/jog.2021.89, 2021.
 - Walter, J. I., Box, J. E., Tulaczyk, S. M., Brodsky, E. E., Howat, I. M., Ahn, Y., and Brown, A. A.: Oceanic mechanical forcing of a marine-terminating Greenland glacier, Annals of Glaciology, 53, 181 192, https://doi.org/10.3189/2012aog60a083, 2012.
 - Werder, M. A., Hewitt, I. J., Schoof, C. G., and Flowers, G. E.: Modeling channelized and distributed subglacial drainage in two dimensions, Journal of Geophysical Research: Earth Surface, 118, 2140–2158, https://doi.org/https://doi.org/10.1002/jgrf.20146, 2013.
- Wood, M., Rignot, E., Fenty, I., An, L., Bjørk, A., van den Broeke, M., Cai, C., Kane, E., Menemenlis, D., Millan, R., et al.: Ocean forcing drives glacier retreat in Greenland, Science Advances, 7, eaba7282, https://doi.org/10.1126/sciadv.aba7282, 2021.
 - Zhang, E.: Compounding seasonal variations in outlet glacier dynamics revealed by high-resolution observations, https://doi.org/10.5281/zenodo.8428196, 2023.
- Zhang, E., Catania, G., and Trugman, D. T.: AutoTerm: an automated pipeline for glacier terminus extraction using machine learning and a "big data" repository of Greenland glacier termini, The Cryosphere, 17, 3485–3503, https://doi.org/10.5194/tc-17-3485-2023, 2023.